

Large-scale heterogeneity of Amazonian phenology revealed from 26-year long AVHRR/NDVI time-series

This article has been downloaded from IOPscience. Please scroll down to see the full text article.

2013 Environ. Res. Lett. 8 024011

(<http://iopscience.iop.org/1748-9326/8/2/024011>)

View [the table of contents for this issue](#), or go to the [journal homepage](#) for more

Download details:

IP Address: 150.163.34.9

The article was downloaded on 12/07/2013 at 17:34

Please note that [terms and conditions apply](#).

Corrigendum: Large-scale heterogeneity of Amazonian phenology revealed from 26-year long AVHRR/NDVI time-series

2013 *Environ. Res. Lett.* **8** 024011

Fabrício B Silva¹, Yosio E Shimabukuro¹, Luiz E O C Aragão^{1,2},
Liana O Anderson^{1,3}, Gabriel Pereira¹, Franciele Cardozo¹ and
Egídio Arai¹

¹ National Institute for Space Research, Avenida dos Astronautas 1758, São José dos Campos-SP, Brazil

² College of Life and Environmental Sciences, University of Exeter, Exeter EX4 4RJ, UK

³ Environmental Change Institute, University of Oxford, South Parks Road, Oxford OX1 3QY, UK

E-mail: fabricaoagro@gmail.com and laragao@dsr.inpe.br

Received 3 May 2013

Accepted for publication 8 May 2013

Published 20 May 2013

Online at stacks.iop.org/ERL/8/029502

There is an error in figure 7; figure 7(a) is the same as figure 6(a). The corrected figure and caption are given below.



Content from this work may be used under the terms of the [Creative Commons Attribution 3.0 licence](https://creativecommons.org/licenses/by/3.0/). Any further distribution of this work must maintain attribution to the author(s) and the title of the work, journal citation and DOI.

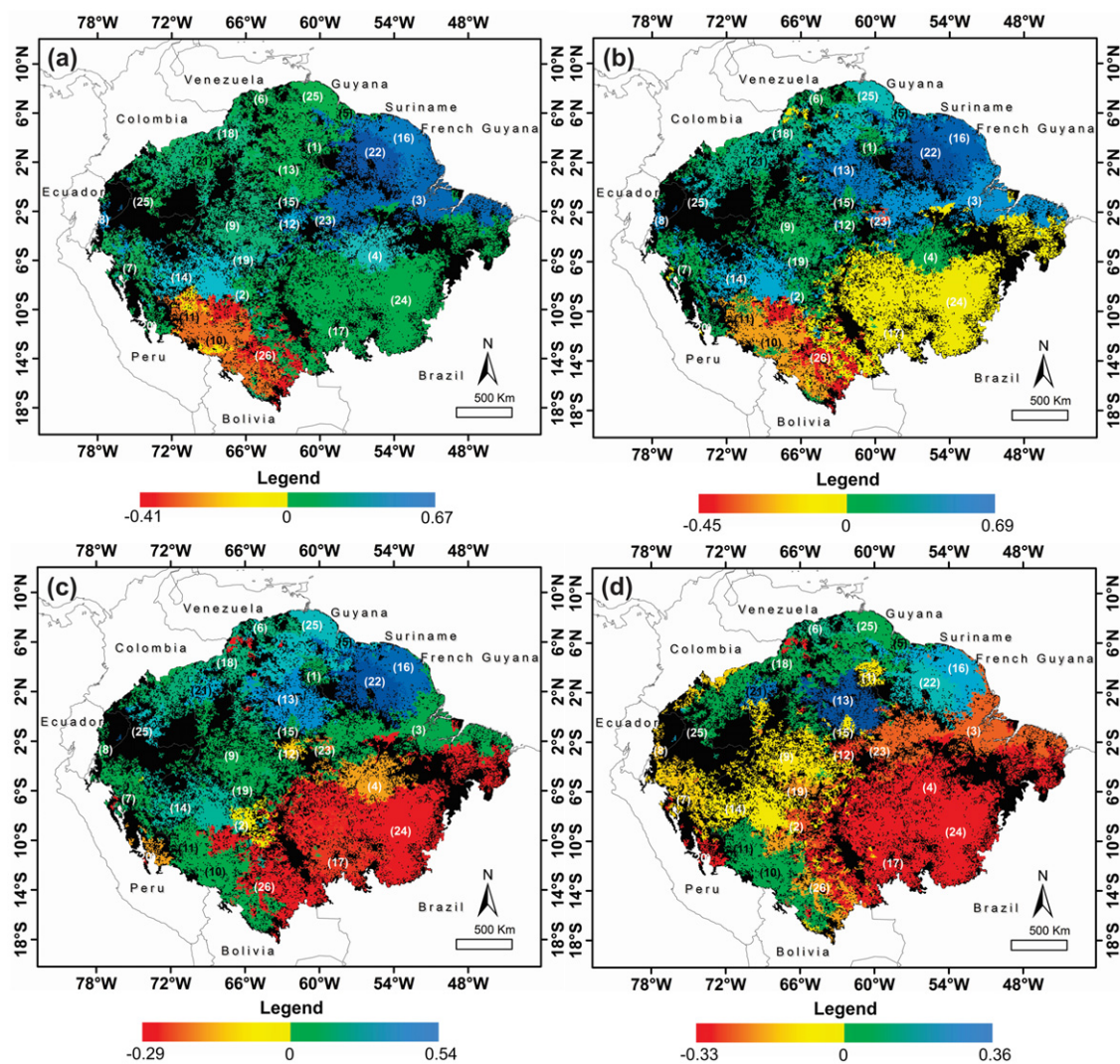


Figure 7. Pearson correlation coefficient between NDVI and incoming radiation (a) without lag, (b) with 1-month lag, (c) with 2-month lag and (d) with 3-month lag. The black color corresponds to unclassified areas in the phenoregion map (see figure 1).

Large-scale heterogeneity of Amazonian phenology revealed from 26-year long AVHRR/NDVI time-series

Fabrício B Silva¹, Yosio E Shimabukuro¹, Luiz E O C Aragão^{1,2},
Liana O Anderson^{1,3}, Gabriel Pereira¹, Franciele Cardozo¹ and
Egídio Arai¹

¹ National Institute for Space Research, Avenida dos Astronautas 1758, São José dos Campos-SP, Brazil

² College of Life and Environmental Sciences, University of Exeter, Exeter EX4 4RJ, UK

³ Environmental Change Institute, University of Oxford, South Parks Road, Oxford, OX1 3QY, UK

E-mail: fabricaoagro@gmail.com and laragao@dsr.inpe.br

Received 1 February 2013

Accepted for publication 25 March 2013


Published 18 April 2013

Online at stacks.iop.org/ERL/8/024011

Abstract

Depiction of phenological cycles in tropical forests is critical for an understanding of seasonal patterns in carbon and water fluxes as well as the responses of vegetation to climate variations. However, the detection of clear spatially explicit phenological patterns across Amazonia has proven difficult using data from the Moderate Resolution Imaging Spectroradiometer (MODIS). In this work, we propose an alternative approach based on a 26-year time-series of the normalized difference vegetation index (NDVI) from the Advanced Very High Resolution Radiometer (AVHRR) to identify regions with homogeneous phenological cycles in Amazonia. Specifically, we aim to use a pattern recognition technique, based on temporal signal processing concepts, to map Amazonian phenoregions and to compare the identified patterns with field-derived information. Our automated method recognized 26 phenoregions with unique intra-annual seasonality. This result highlights the fact that known vegetation types in Amazonia are not only structurally different but also phenologically distinct. Flushing of new leaves observed in the field is, in most cases, associated to a continuous increase in NDVI. The peak in leaf production is normally observed from the beginning to the middle of the wet season in 66% of the field sites analyzed. The phenoregion map presented in this work gives a new perspective on the dynamics of Amazonian canopies. It is clear that the phenology across Amazonia is more variable than previously detected using remote sensing data. An understanding of the implications of this spatial heterogeneity on the seasonality of Amazonian forest processes is a crucial step towards accurately quantifying the role of tropical forests within global biogeochemical cycles.

Keywords: tropical forest, vegetation index, Amazonia, phenology, leaf flushing, remote sensing

 Online supplementary data available from stacks.iop.org/ERL/8/024011/mmedia



Content from this work may be used under the terms of the [Creative Commons Attribution 3.0 licence](http://creativecommons.org/licenses/by/3.0/). Any further distribution of this work must maintain attribution to the author(s) and the title of the work, journal citation and DOI.

1. Introduction

Forest phenology is a critical process regulating fluxes of carbon and water between the biosphere and the atmosphere.

Biophysical and structural changes in the forest canopy driven by phenological cycles are closely tied to vegetation–climate feedbacks (Richardson *et al* 2013, Wu *et al* 2012, Gonsamo *et al* 2012). Therefore, depiction of the spatial configuration of phenological cycles in multiple biomes is essential for improvement of the representation of ecophysiological processes in Earth system models (Bradley *et al* 2011) and for evaluation of the impacts of climatic variation on these processes (Richardson *et al* 2013).

Undisturbed Amazonian vegetation is characterized by a heterogeneous mosaic of forest types (Silman 2007, Gond *et al* 2011) originating from complex interactions between three main factors: (1) climate, which generates gradients in the timing of the onset and ending of the dry season (Liebmann and Marengo 2001, Sombroek 2001), the length of the dry season (Marengo *et al* 2001) and the seasonality of solar radiation (Schafer *et al* 2002); (2) environmental factors, which present a large heterogeneity in soil physical and chemical characteristics (Quesada *et al* 2009), drainage and topography; and (3) biological factors, which are characterized by changes in species composition across the basin (Sombroek 2001, Sternberg 2001, ter Steege *et al* 2006), by structural differences in canopy sizes (Barbier *et al* 2009), by gradients of net primary productivity (Aragão *et al* 2009) and by canopy litter production (Chave *et al* 2010).

Previous studies using the normalized difference vegetation index (NDVI) derived from Advanced Very High Resolution Radiometer (AVHRR) data have shown little variation in the phenology of Amazonian forests (Batista *et al* 1997, Maignan *et al* 2008). Distinct changes in the amplitude of the NDVI, however, were observed for eastern (high amplitude) and north-western (low amplitude) Amazonia (Asner *et al* 2000). Negative anomalies in the NDVI during the dry season of eastern Amazonia were associated with decreases in canopy greenness related to dry season water stress. Moreover, the reduction in the amplitude of the NDVI from El Niño to La Niña years suggested that Amazon forest phenology is responsive to rainfall variations. Further research analyzing vegetation index (VI) and leaf area index (LAI) products derived from MODIS data have advanced our knowledge on the phenology of Amazonian forests (Huete *et al* 2006, Myneni *et al* 2007, Xiao *et al* 2006, Saleska *et al* 2007, Anderson *et al* 2010, Brando *et al* 2010, Anderson *et al* 2011, Bradley *et al* 2011, Samanta *et al* 2012). An important breakthrough using MODIS data was the identification of seasonal changes in forest greening during the dry season as a response to increased solar radiation for large areas of primary forests in Amazonia (Huete *et al* 2006, Myneni *et al* 2007, Xiao *et al* 2006, Samanta *et al* 2012). However, generalization of the dry season green up over Amazonian forests must be interpreted cautiously. Bradley *et al* (2011), using similar data, showed that 1.27×10^6 km² of the forested area analyzed was in phase with radiation, while 1.58×10^6 km² was in phase with precipitation. Most of the forested area had a weak seasonality (Bradley *et al* 2011). Moreover, inter-annual variability in changes in the VI could not be explained by climatic variation in Amazonia (Brando *et al* 2010). This variability indicates

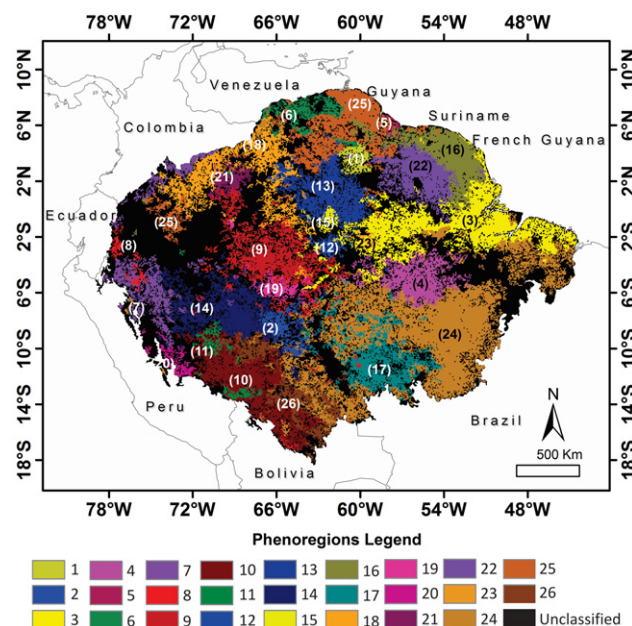


Figure 1. Phenoregions identified in the Amazon basin.

that other environmental controls may play an important role in determining the phenology of Amazonian forests. Our knowledge about Amazonian phenology is still limited to basin-wide generalizations, mainly because of unsuccessful attempts to identify spatially variable coherent regional patterns of phenology. This is in part due to limitations linked to the length of the time-series available for previous analysis (<10 yr) and field information confined to a single area in eastern Amazonia (Tapajós National Forest; Doughty and Goulden 2008, Malhado *et al* 2009, Brando *et al* 2010) that may not be representative of other areas of Amazonia, and therefore limiting our capacity to interpret the patterns observed from satellite data.

Based on the principle that phenological variation of tropical trees is shaped through adaptations to biotic and abiotic factors and, hence, phenological traits are an evolutionary reflection of the influence of these external factors (van Schaik *et al* 1993, Borchert 1994, Borchert *et al* 2002), we expect that the phenological cycles within Amazonian vegetation types will vary greatly, reproducing the environmental diversity that can emerge from the spatial arrangement of potential drivers of phenology identified above for this biome. Despite the difficulty in determining the ultimate causes of forest phenological cycles, analysis of pixel-based long-term seasonality of VI is likely to provide an indication of spatially explicit homogenous phenological responses of Amazonian vegetation to different evolutionary pressures. The longest satellite-derived VI time-series currently available is the NDVI from AVHRR (1981–2011) (Zhu *et al* 2013). A recent comparison between the NDVI and the enhanced vegetation index (EVI) from MODIS revealed that bidirectional reflectance effects are more exacerbated in the EVI than the NDVI, potentially influencing the interpretation of phenological cycles in forest ecosystems (Galvão *et al* 2011).

Table 1. Vegetation description, dry season period (monthly precipitation < 100 mm), peak of maximum NDVI and proportional variation of NDVI for all phenoregions.

Phenoregion	Vegetation description	Reference	Dry season	Peak of maximum NDVI	% NDVI variation (max–min)
1	Roraima savanna	IBGE (2004)	Oct–Mar	Aug	31.71
2	Dense forest of low lands with lianas	IBGE (2004)	Jun–Sep	Jul	25.19
3	Alluvial dense evergreen forest in low lands	IBGE (2004)	Aug–Nov	Aug	21.72
4	Dense forest of low lands	IBGE (2004)	Jul–Oct	Jul	36.33
5	Low land dense moist forest	Selvaradjou <i>et al</i> (2005)	Jan–Mar	Sep	20.11
6	Savanna	Panagos <i>et al</i> (2011)	Nov–Apr	Sep	22.14
7	Andes–Amazon transition forest	Panagos <i>et al</i> (2011)	Jul–Sep	Sep	20.29
8	Premontane pluvial forest	Panagos <i>et al</i> (2011)	May–Sep	Aug	30.97
9	Closed evergreen forest	IBGE (2004)	Jun–Oct	Aug	17.93
10	Evergreen forest in high lands	Panagos <i>et al</i> (2011)	Jun–Ago	Jun	18.13
11	Bamboo forest	IBGE (2004)	May–Sep	Jul	21.65
12	Dense forest of low lands with palms	IBGE (2004)	Aug–Oct	Aug	25.76
13	Campinarana forest	IBGE (2004)	Aug–Oct	Nov	20.09
14	Low lands evergreen open forest	IBGE (2004)	Jun–Ago	Jul	20.78
15	Campinarana forest with palms and shrubs	IBGE (2004)	Oct–Jan	Oct	22.12
16	High forest with regular canopy	Huber (2006)	Aug–Oct	Sep	30.38
17	Submontane forest with palms and lianas	IBGE (2004)	May–Sep	Jul	27.81
18	Pluvial forest in high lands	Panagos <i>et al</i> (2011)	Dec–Feb	Dec	16.67
19	Dense evergreen forest with palms and lianas	IBGE (2004)	Jun–Sep	Aug	24.43
20	Premontane dry forest	Panagos <i>et al</i> (2011)	Jun–Sep	Aug	29.15
21	Xerophytic vegetation	Rangel <i>et al</i> (1997)	Jun–Oct	Dec	24.50
22	Mixed high and open forest with a tropical savanna climate	Gond <i>et al</i> (2011)	Dec–Mar	Sep	39.07
23	Dense evergreen forest in low lands with palms and lianas	IBGE (2004)	Aug–Nov	Jul	25.30
24	Forest transition between dense, open forest and savanna	IBGE (2004)	Jun–Sep	Jun	23.56
25	Mosaic of evergreen lowland forest, swamp forest, and savanna	Anhuf and Winkler (1999)	Dec–Mar	Oct	16.52
26	Flooded savanna	López and Zambrana-Torrelío (2005)	Jun–Sep	Apr	22.46

To identify distinct ecological responses of Amazonian forests to localized biotic and abiotic controls, in this study we propose to analyze 26-year long time-series of NDVI data from AVHRR using a novel pixel-level pattern recognition technique based on temporal signal processing concepts. Specifically, we aim to (1) characterize the spatial variability of forest phenology in Amazonia by identifying regions where the forest phenological cycle is homogeneous (phenoregions); (2) quantify the relationships between the seasonality of the NDVI signal of each distinct phenoregion and climate by analyzing the covariance between NDVI, rainfall and solar radiation; and finally (3) investigate how the NDVI changes in relation to field-derived data on leaf flushing and litterfall

based on a new compilation of published information for Amazonia.

2. Material and methods

2.1. Datasets

We used two long-term NDVI time-series (1982–2008) with 8 km spatial resolution from the Advanced Very High Resolution Radiometer (AVHRR) available from the Global Inventory Monitoring and Modeling Studies (GIMMS) group. The first corresponds to biweekly data and the second to monthly data. These two datasets have been

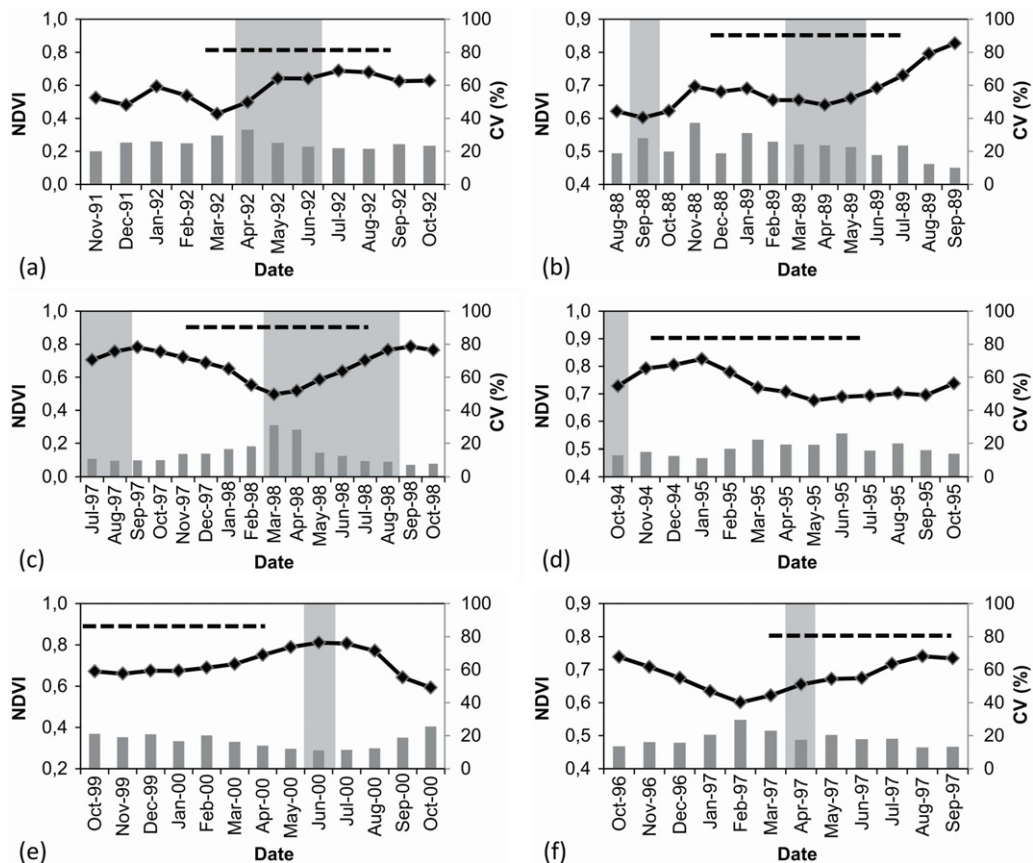


Figure 2. Comparison between phenoregions' NDVI time-series (—◆—). Production peak of new leaves (shaded). Monthly coefficient of variation of NDVI (vertical bars) and rainy season (dashed line). (a) Phenoregion 6 (Norconk and Conklin-Brittain 2004); (b) Phenoregion 9 (Peres 1994); (c) Phenoregion 16 (Bonal *et al* 2000); (d) Phenoregion 18 (Boubli 2005); (e) Phenoregion 24 (Pinto and Setz 2004); (f) Phenoregion 25 (Basset *et al* 2001).

constantly improved to minimize noise resulting from residual atmospheric effects, orbital drift, inter-sensor variations, and stratospheric aerosol effects (Tucker *et al* 2005, Pinzon *et al* 2005). The biweekly data were used for the pattern recognition analysis due to their higher temporal resolution. The monthly data were used to perform the correlation analysis between monthly rainfall and incoming radiation and NDVI datasets, as well as to investigate the seasonality of field phenology, NDVI and rainfall data.

Monthly precipitation and incoming radiation time-series covering the period from 2000 to 2008 were created for each phenoregion based on the Global Land Data Assimilation System (GLDAS) precipitation grids (0.25° spatial resolution) (Rodell *et al* 2004). Additionally, we compiled published information on field observations of peak of new leaf and litterfall production for 12 sites in Amazonia to investigate how the NDVIs for selected phenoregions respond to the seasonality of these two phenological processes: (1) leaf flushing and (2) abscission (table S1 available at stacks.iop.org/ERL/8/024011/mmedia).

To reduce the effect of land use and land cover change on the phenological signal, we masked all areas corresponding to agriculture, water body, bare soil and urban areas based on the GLOBCOVER product developed by the European Space Agency (ESA) (Arino *et al* 2007).

2.2. Data processing

Our rationale for detecting forest phenology was based on three assumptions: (1) NDVI time-series can provide cyclical spectra that are directly related to the distinct phenological patterns of each phenoregion; (2) the periodicity of the cycles can be mathematically separated, allowing the identification of phenologically homogenous regions; and (3) the multi-temporal nature of the NDVI time-series is analogous to the characteristics of hyperspectral data, permitting the use of similar image processing techniques.

We applied a signal processing approach to the NDVI time-series aiming to automatically identify NDVI standard curves, which represent phenological forest patterns, in order to map these regions. This signal processing approach consisted of 'noise-adjusted' principal component analysis (minimum noise fraction), automated extraction of end members (pixel purity index) and an automated classification method based on spectral similarity (spectral angle mapper).

The minimum noise fraction (MNF) is a linear transform that provides an optimal ordering of images in terms of image quality and increases the signal to noise ratio, generating principal component images that are unaffected by noise (Green *et al* 1988).

After MNF transformation, the pixel purity index (PPI) was then applied to the principal component images. The

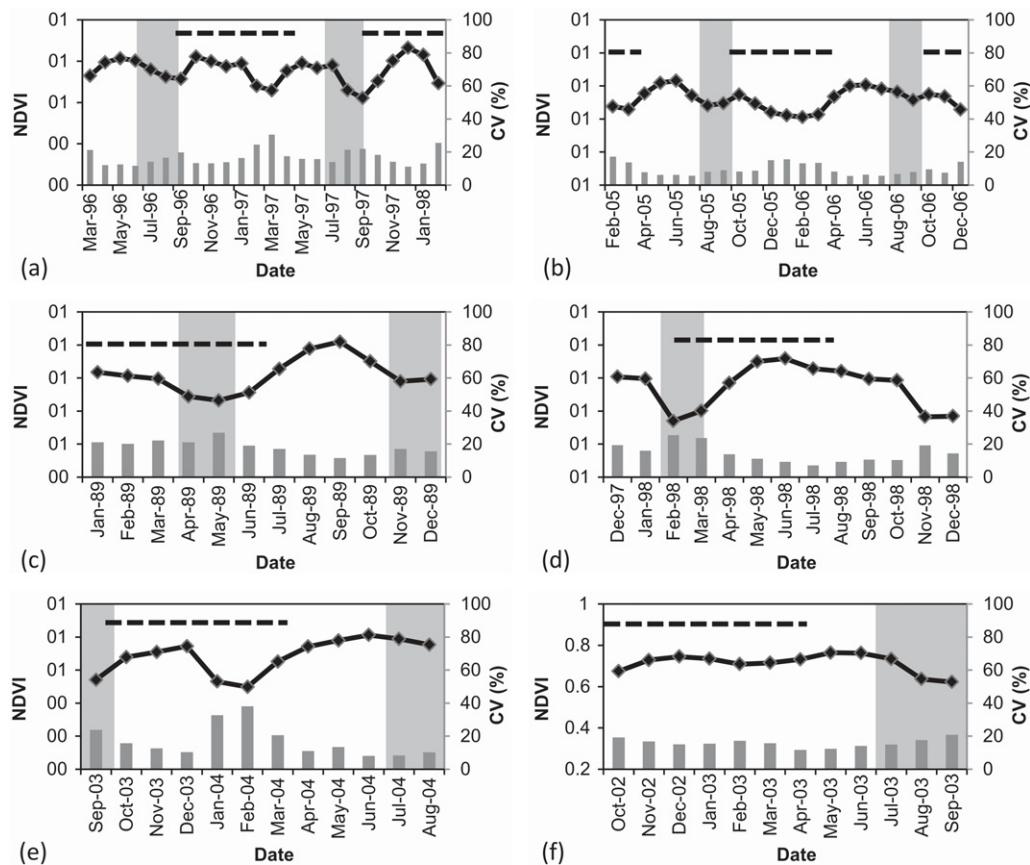


Figure 3. Comparison between phenoregions' NDVI time-series (—◆—). Production peak of litterfall (shaded). Monthly coefficient of variation of NDVI (vertical bars) and rainy season (dashed line). (a) Phenoregion 10 (Justiniano and Fredericksen 2000); (b) Phenoregion 11 (RAINFOR—Tambopata Site); (c) Phenoregion 13 (Barbosa and Fearnside 1996); (d) Phenoregion 14 (Nebel *et al* 2001); (e) Phenoregion 17 (Selva *et al* 2007); (f) Phenoregion 26 (Brienen and Zuidema 2005).

PPI is an algorithm based on convex geometry concepts used to find the most 'spectrally pure' or extreme pixels (end members), which examines multidimensional envisioned data in n -dimensions. Each point (pixel) within this data space can be examined as a linear combination of an unknown number of pure components (Boardman 1995). The PPI is computed by repeatedly projecting n -dimensional scatter plots onto a random unit vector. The extreme pixels in each projection are recorded and the total number of times each pixel is marked as extreme is noted. A threshold of 5000 pixels was used to define how many pixels are marked as extreme at the end of the projected vector.

The selected end members (phenological signatures) were then used as input for the spectral angle mapper (SAM) analysis. This pattern recognition technique is based on the measurement of spectral similarity between two or more spectra obtained considering each spectrum as a vector in n -dimensional space (Kruse *et al* 1993). Once similar spectra are identified they are aggregated into a single category. Lastly, the resulting map was postprocessed and pixels with less than nine neighbors and phenoregions with less than 100 pixels were excluded from the final map.

We computed for each phenoregion the mean monthly NDVI. These time-series were smoothed using the Savitzky–Golay filter (Chen *et al* 2004) and the coefficient of variation

was calculated as a homogeneity index. For each NDVI time-series extracted from each phenoregion, phenophases corresponding to the start (SS), end (ES) and peak (PS) of the growing season were calculated according to the methodology proposed by Jönsson and Eklundh (2002).

Finally, correlation analyses were performed to quantify the relationships between NDVI and rainfall and radiation for each phenoregion.

3. Results and discussion

The pattern recognition technique enabled the characterization of 26 phenoregions with distinct long-term NDVI temporal cycles (figure 1). These phenoregions tended, in general, to reflect the spatial distribution of main vegetation types described for Amazonia (table 1).

Previous studies used approaches based on automated cluster analysis or training techniques using multisensor data (Saatchi *et al* 2000, Eva *et al* 2003) that do not incorporate the temporal component of phenology dynamics. Consequently, the resulting maps tended to represent Amazonia as a homogeneous lowland humid forest. Conversely, our technique captured the differences between high forest with regular canopy and mixed high and open forest with a tropical savanna climate in the Guyana shield. These two

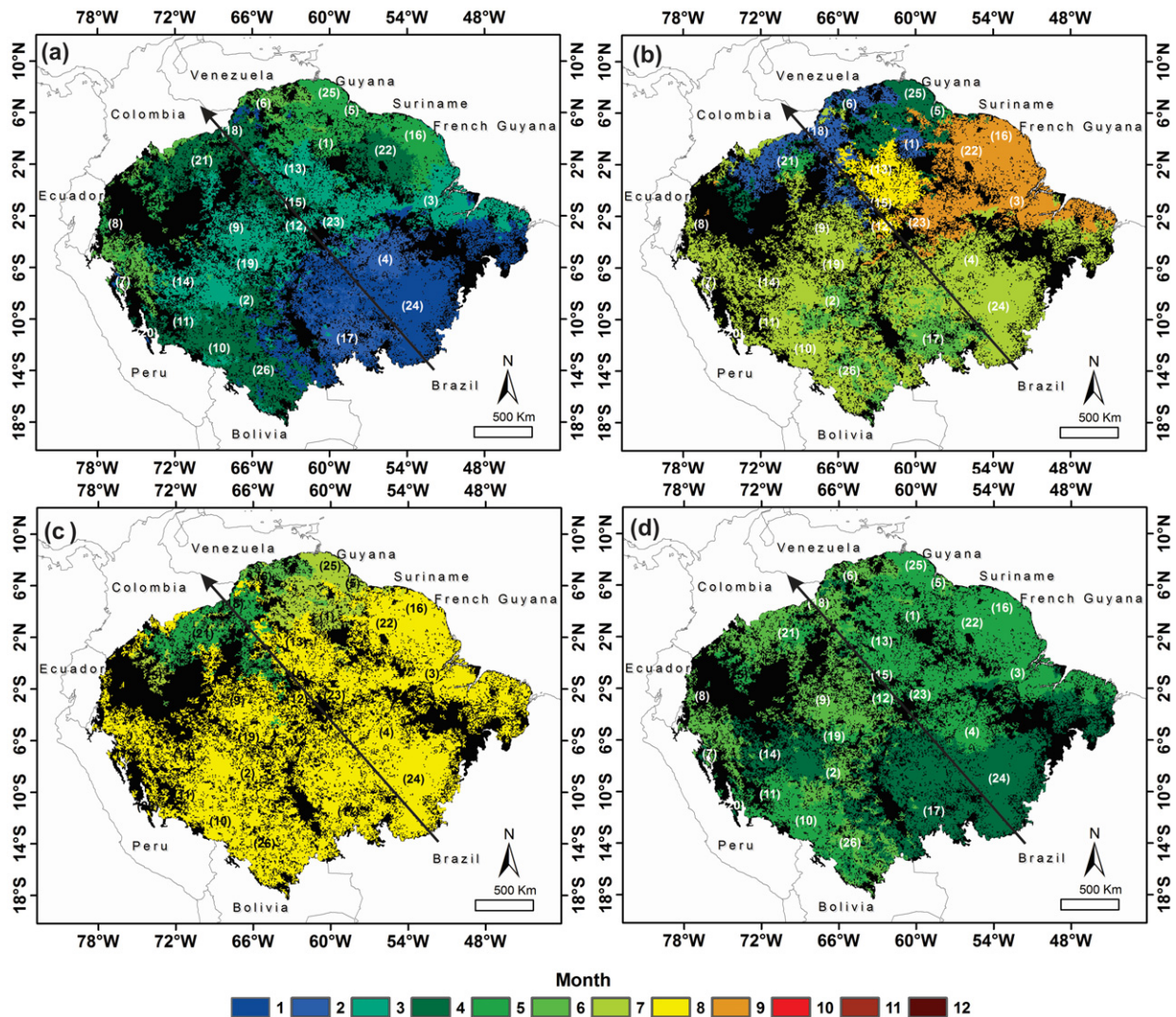


Figure 4. (a) Peak of rainy season, (b) peak of dry season, (c) month of maximum radiation and (d) month of minimum radiation. The arrows indicate the southeast–northwest direction of the climatic gradient. The black color corresponds to unclassified areas in the phenoregion map (see figure 1).

forest types have structural and climate differences that have been previously described (Sombroek 2001, Gond *et al* 2011) but not yet clearly separated using remote sensing data. Another important distinction, probably influenced by climatic gradients, was observed among dense forest, open forest and dry forest in the north–south direction.

3.1. Reconciling NDVI variation with field-based phenology

For all phenoregions analyzed, the peak of new leaf production reported from field observations was followed by a steady increase in NDVI or occurred during the maximum NDVI (figure 2). The peak of litterfall production corresponded to time periods in which NDVI had a descending trend (figure 3).

In contrast to previous studies using MODIS data that reported widespread leaf flushing during the dry season in Amazonia (Huete *et al* 2006, Myneni *et al* 2007, Xiao *et al* 2006, Samanta *et al* 2012), field-based information from our

literature compilation revealed that the peak of new leaf production occurs during the wet season in 66% of the sites. The NDVI from the AVHRR follows this same dynamics with values increasing from the beginning or middle of the rainy season to the end.

Specifically, field-based reports showed that the pluvial forest in high lands (Phenoregion 18) and forest transition between dense, open forest and savanna (Phenoregion 24) presented just one annual peak of new leaf flushing in the dry season (Boublil 2005, Pinto and Setz 2004). The closed evergreen forest (Phenoregion 9) presented two peaks of flushing in the wet season (Peres 1994). The savanna forest (Phenoregion 6), mosaic of evergreen lowland forest, swamp forest, and savanna (Phenoregion 25) and high forest with regular canopy (Phenoregion 16) presented just one peak of flushing in the wet season (Norconk and Conklin-Brittain 2004, Basset *et al* 2001, Bonal *et al* 2000). The NDVI of each phenoregion followed these events in both the dry and the wet season. The coefficient of variation of the NDVI values did

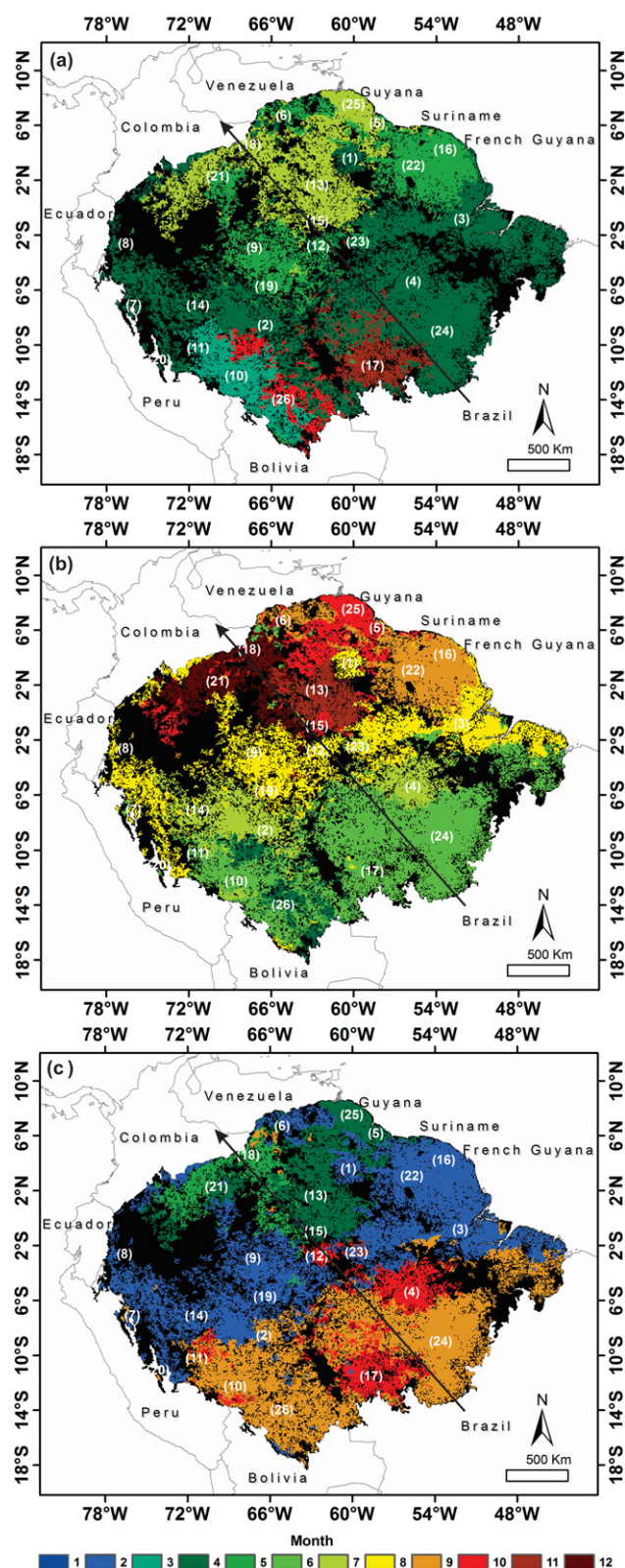


Figure 5. (a) Start of the growing season, (b) peak of the growing season and (c) end of the growing season. The arrows indicate the southeast–northwest direction of the phenology gradient. The black color corresponds to unclassified areas in the phenoregion map (see figure 1).

not exceed 40% in any of the regions analyzed. The automated PPI method captured NDVI temporal signatures consistently with the main phenological features observed in the field.

3.2. Timing of phenological phases

We identified a strong rainfall and radiation gradient, with maximum rainfall occurring in parallel with minimum radiation. Both variables followed a southeast–northwest direction. The phenophases clearly followed this climatic gradient (figure S2 available at stacks.iop.org/ERL/8/024011/mmedia). In the northwest of the basin the onset of the growing season occurred mainly between May and July (figure 5(a)), during the middle to the end of the dry season when solar radiation is at its maximum (figure 4(c)). This region is characterized by a non-existent or short dry season. On the other hand, in the central-north Amazon the onset of the growing season occurred from March through May, during the middle to the end of the wet season, following the increased availability of solar radiation. In the extreme south of the Amazon basin, Phenoregions 17 and 26, characterized by submontane forest and savanna, respectively, had the onset of the growing season between October and December, two months before the maximum rainfall (beginning of the wet season). In the southwest–northeast direction the peak of the growing season (figure 5(b)) occurred following the middle-to-end of wet season gradient, from April (southwest) to September (northeast). The end of the growing season (figure 5(c)) also followed the end of dry season gradient in the southwest–northeast direction (September–February) with a lag of about three months.

Correlation analysis revealed that without lags only savanna forests presented positive correlation with rainfall. However, 76.9% of all phenoregions had a significant positive correlation between NDVI and rainfall with a three month time lag (figure 6). The correlation between NDVI and incoming radiation was positive in a large part of the basin without lags (figure 7). These results indicate that large areas of Amazonian forests strategically flush new leaves from the middle to the end of the wet season when incoming radiation is increasing and soil water availability is still high (Juárez *et al* 2007). A delay effect of the NDVI in response to rainfall is expected and is likely to explain the occurrence of negative correlation coefficients when lags are not considered. An exception was savanna forest and submontane forest with palms and lianas that presented positive correlation between NDVI and rainfall without time lags.

The NDVI amplitude between maximum and minimum values reached 16.67% in the mosaic of evergreen lowland forest, swamp forest, and savanna (Phenoregion 22) and 39.07% in the mixed high and open forest with a tropical savanna climate (Phenoregion 25). In the alluvial dense evergreen forest domain in the low lands (Phenoregion 3), where Tapajos National Forest and Caxiuanã National Forest are located, the NDVI amplitude reached 21.72% (table S1 available at stacks.iop.org/ERL/8/024011/mmedia). These results were similar to previous studies that used EVI (Samanta *et al* 2012, Myneni *et al* 2007, Huete *et al* 2006).

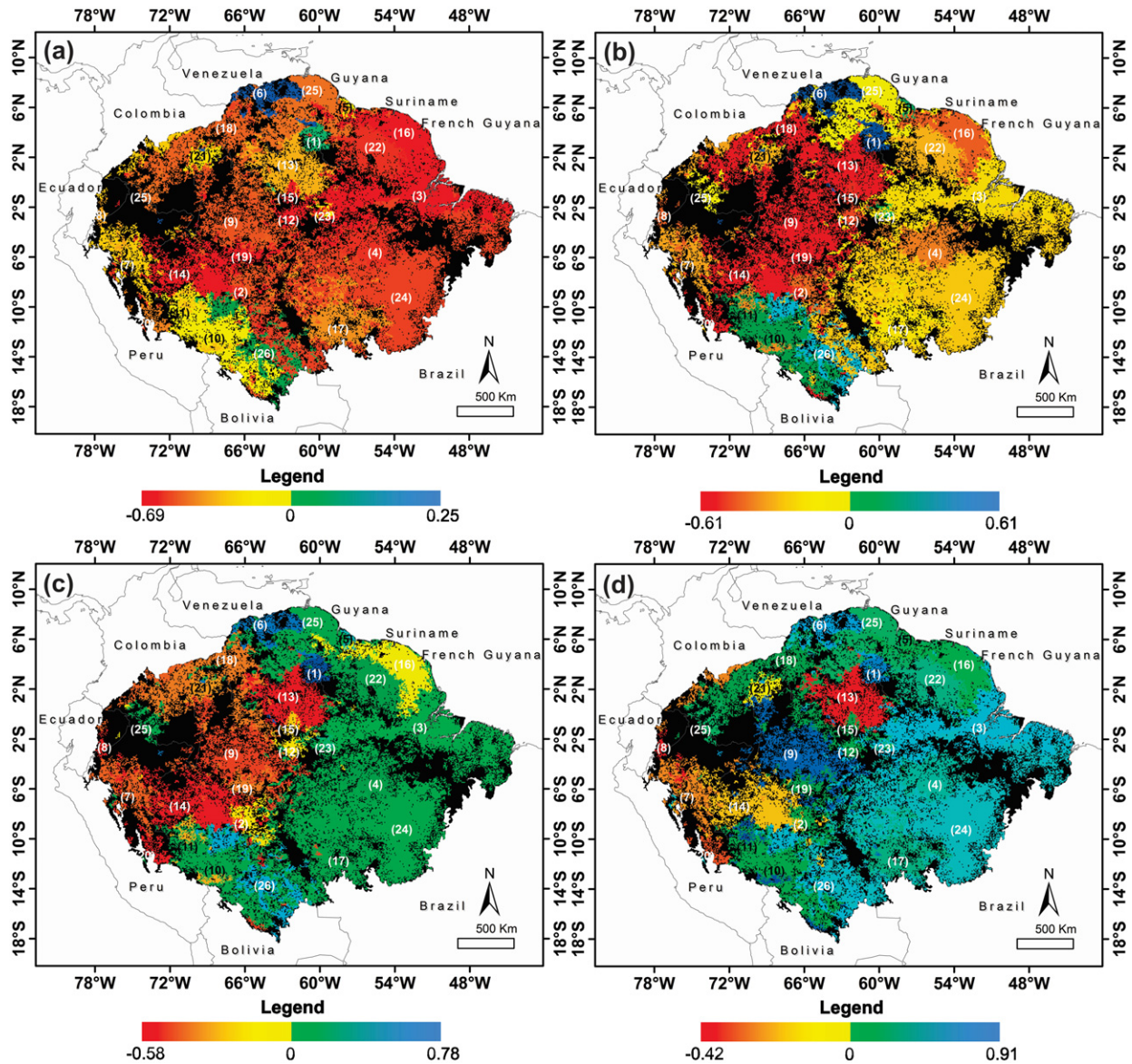


Figure 6. The Pearson correlation coefficient between NDVI and precipitation (a) without lag, (b) with one month lag, (c) with two month lag and (d) with three month lag. The black color corresponds to unclassified areas in the phenoregion map (see figure 1).

Our results showed a basin-wide phenological gradient delay between the southeast and northwest portions of four months for the start of the growing season and six months for the peak of growing season, when the forest reached the highest NDVI values at the middle-to-end of the wet season. This reveals that the phenological responses to climatic variation are heterogeneous across Amazonia. Based on our NDVI and field-based analysis we argue that the flush of new leaves does not occur simultaneously during the dry season across all Amazonian forest as previously stated (Samanta *et al* 2012, Myneni *et al* 2007, Saleska *et al* 2007, Huete *et al* 2006, Asner *et al* 2004). By combining the long-term NDVI time-series (26 years) with ground-based studies produced in the last 26 years, we highlighted that leaf flushing in the majority of Amazonia, as approximated by the NDVI, starts after the soil is fully recharged with water and incoming

radiation starts to increase after the peak of the wet season. This tendency is characterized in our data by a peak in the NDVI by the end of the rainy season. We demonstrated that the onset and end of the growing seasons in Amazonia cannot be considered to occur simultaneously throughout the basin from July to September. We showed a southeast–northwest direction gradient of rainy and dry seasons (figures 4 and 5). It was also possible to note a difference of five months in the peaks of the dry and wet seasons in the southeast–northwest direction and four months in the start of the growing season (September to December) in the west–east direction of the Amazon basin, which is in agreement with Marengo *et al* (2001).

It is interesting to note that in a large fraction of southern Amazonia, the growing season occurs almost exclusively during the wet season for a period of three months. In contrast,

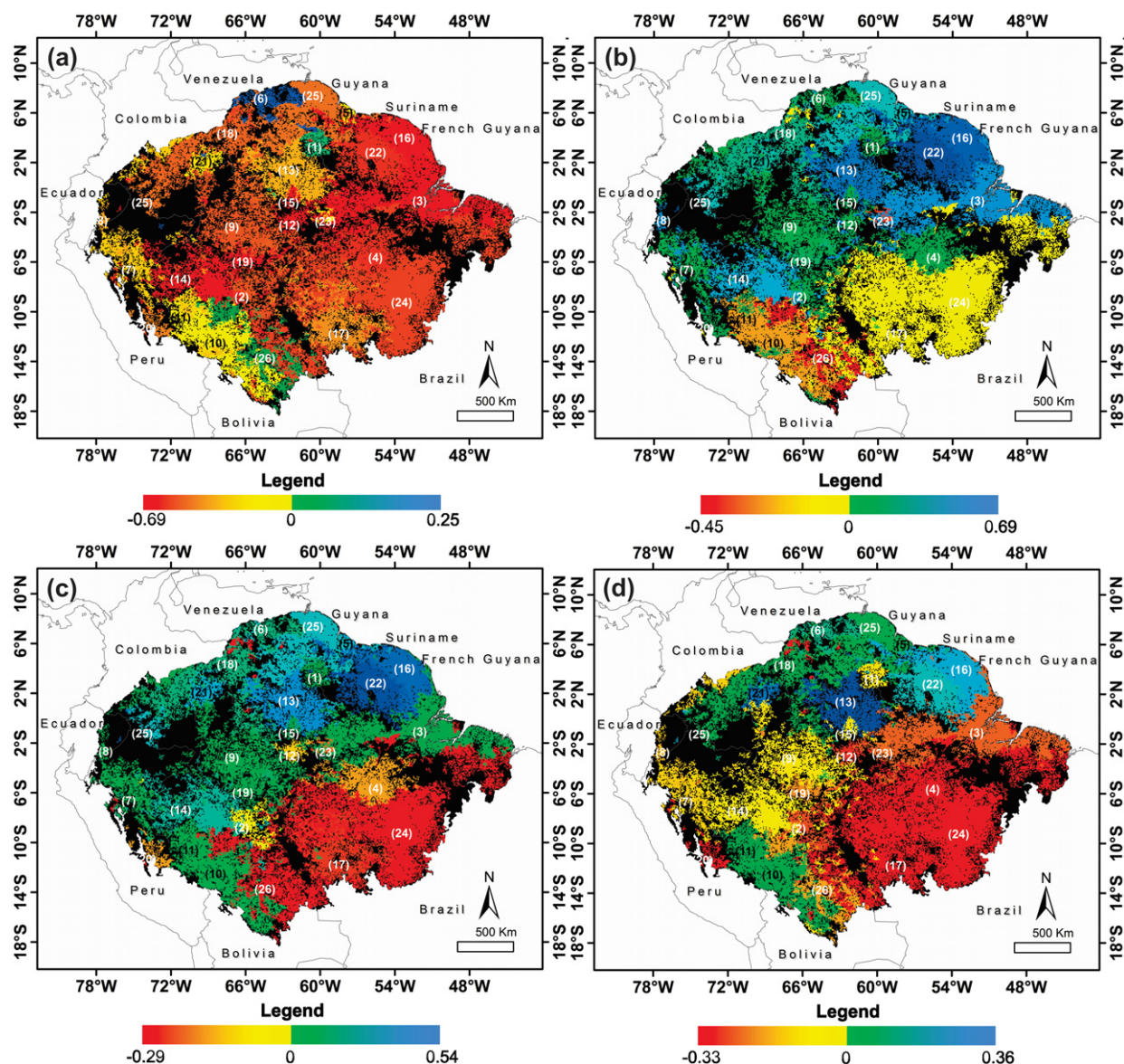


Figure 7. The Pearson correlation coefficient between NDVI and incoming radiation (a) without lag, (b) with one month lag, (c) with two month lag and (d) with three month lag. The black color corresponds to unclassified areas in the phenoregion map (see figure 1).

in the northern, and wetter, fraction of the basin the growing season occurs during the transition between wet and dry seasons for a period of six months. The shorter time of the growing season in the south could be associated with a ‘sprint’ of greenness as an evolutionary strategy to reduce losses through herbivory during this susceptible phase of foliar development (Patino *et al* 2012, Moles and Westoby 2000). This ‘sprint’ of greenness could be either associated to the flushing of new leaves (Sinimbu *et al* 2012) or to the increased rate of leaf expansion (Brando *et al* 2010).

Previous studies of Amazonia greening tend to assume a dry season between July and October, concluding that Amazonia greens up during the dry season (Samanta *et al* 2012, Huete *et al* 2006, Xiao *et al* 2006). Therefore, due to the variability observed here in the timing of phenological phases and climatic gradient, more caution should be taken when linking climatic conditions with canopy phenology in Amazonia.

4. Conclusions

This work provided a critical understanding of the phenological mosaics in Amazonia and how they respond to climatic variability. The fundamental aspect of our methodology was the implementation of a pixel by pixel pattern recognition technique that could successfully identify the differences in the natural cycles of forest phenology. Our phenoregion map clearly distinguishes regions that were not detected in previous studies. This is probably because spatially pixels are spectrally similar but temporally they produce distinct responses to biotic and abiotic factors.

Differently from previous studies, using MODIS data, which generated contradictory results, creating an unresolvable debate (Saleska *et al* 2007, Asner and Alencar 2010, Samanta *et al* 2012, Atkinson *et al* 2011), our results added a new and independent perspective on the phenology of Amazonian forests. The coherent phenological patterns found

in our analysis are a result of the combination of the data characteristics and the methodological approach used. In spite of inherent limitations of optical remote sensing, in terms of saturation of NDVI signal over tropical canopies (Aragão *et al* 2005) and interference of clouds (Asner and Alencar 2010), it appears that, in particular, the length of the time-series allowed the detection of cyclical behavior in the AVHRR/NDVI data. This indicates that saturation of NDVI was not a problem for the analysis. Moreover, the identification of peak NDVI during the dry season in some areas and the wet season in other areas indicates that cloud cover is not a major factor influencing the seasonality of this dataset. Because our methodology explicitly distinguishes curves based on their shape and not their amplitude, the influence of NDVI saturation and potential cloud or aerosol interference is minimized.

Forest phenology is a complex process involving several environmental factors which enables similar vegetation types to develop distinct phenological cycles or, alternatively, different vegetation types to develop similar phenological cycles. For this reason we opted to compare the phenoregions with the main vegetation types on a macroscale.

Our results show that Amazon forest phenology is more heterogeneous than previously anticipated. To better understand the drivers of this heterogeneity it is critical to perform a formal evaluation of the contribution of other variables across the basin, including soil, geomorphology, vegetation and climatic information.

Acknowledgments

We would like to thank the National Research Council of Brazil (CNPq) for providing the PhD studentship to FBS and the Special Visiting Researcher Fellowship through the program Science Without Borders to LEOCA.

Author contributions

FBS, YES and LEOCA designed the experiment; FBS, GP, FC and EA processed the data; FBS, YES, LEOCA and LOA analyzed the results; FBS and LEOCA wrote the paper.

References

- Anderson L O, Aragão L E O C, Shimabukuro Y E, Almeida S and Huete A 2011 Fraction images for monitoring intra-annual phenology of different vegetation physiognomies in Amazonia *Int. J. Remote Sens.* **32** 387–408
- Anderson L O, Malhi Y, Aragão L E O C, Ladle R, Arai E, Barbier N and Phillips O 2010 Remote sensing detection of droughts in Amazonian forest canopies *New Phytol.* **187** 733–50
- Anhuf D and Winkler H 1999 Geographical and ecological settings of the Surumoni-crane-project (Upper Orinoco, Estado Amazonas, Venezuela) *Anz. Abstr.* **135** 3–23
- Aragão L E O C, Shimabukuro Y E, Espirito-Santo F D B and Williams M 2005 Spatial validation of the collection 4 MODIS LAI product in eastern Amazonia *IEEE Trans. Geosci. Remote Sens.* **43** 2526–34
- Aragão L E O C *et al* 2009 Above- and below-ground net primary productivity across ten Amazonian forests on contrasting soils *Biogeosciences* **12** 2759–78

- Arino O *et al* 2007 GlobCover: ESA service for global land cover from MERIS *IGARSS 2007: IEEE Int. Geoscience and Remote Sensing Symposium* (New York: IEEE) pp 2412–5 (doi:10.1109/IGARSS.2007.4423328)
- Asner G P and Alencar A 2010 Drought impacts on the Amazon forest: the remote sensing perspective *New Phytol.* **187** 569–78
- Asner G P, Nepstad D, Cardinot G and Ray D 2004 Drought stress and carbon uptake in an Amazon forest measured with spaceborne imaging spectroscopy *Proc. Natl Acad. Sci. USA* **101** 6039–44
- Asner G P, Townsend A R and Braswell B H 2000 Satellite observation of El Niño effects on Amazon Forest phenology and productivity *Geophys. Res. Lett.* **27** 981–4
- Atkinson P M, Dash J and Jeganathan C 2011 Amazon vegetation greenness as measured by satellite sensors over the last decade *Geophys. Res. Lett.* **38** L19105
- Barbier E B, Burgess J C and Grainger A 2009 The forest transition: towards a more comprehensive theoretical framework *Land Use Policy* **27** 98–107
- Barbosa R I and Fearnside P M 1996 Carbon and nutrient flows in an Amazonian forest: fine litter production and composition at Apiaú, Roraima, Brazil *Trop. Ecol.* **37** 115–25
- Basset Y, Novotny V, Miller S E and Kitching R 2001 Short-term effects of canopy openness on insect herbivores in a rain forest in Guyana *J. Appl. Ecol.* **38** 1045–58
- Batista G T, Shimabukuro Y E and Lawrence W T 1997 The long-term monitoring of vegetation cover in the Amazonian region of northern Brazil using NOAA-AVHRR data *Int. J. Remote Sens.* **18** 3195–210
- Boardman J W 1995 Analysis understanding and visualization of hyperspectral data as convex sets in *n*-space *Proc. SPIE* **2480** 14–22
- Bonal D, Sabatier D, Montpied P, Tremeaux D and Guehl J M 2000 Interspecific variability of $\delta^{13}\text{C}$ among trees in rainforests of French Guiana: functional groups and canopy integration *Oecologia* **124** 454–68
- Borchert R 1994 Soil and stem water storage determine phenology and distribution of tropical dry forest trees *Ecology* **75** 1437–49
- Borchert R, Rivera G and Hagnauer W 2002 Modification of vegetative phenology in a tropical semi-deciduous forest by abnormal drought and rain *Biotropica* **34** 27–39
- Boublil J P 2005 Floristic, primary productivity and primate diversity in Amazonia: contrasting a eutrophic várzea forest and an oligotrophic caatinga forest in Brazil *Tropical Fruits and Frugivores* ed D J Lawrence and J P Boublil (Dordrecht: Kluwer Academic) pp 59–73
- Bradley A V, Gerard F F, Barbier N, Weedon G P, Anderson L O, Huntingford C, Aragão L E O C, Zelazowski P and Arai E 2011 Relationships between phenology, radiation, and precipitation in the Amazon region *Glob. Change Biol.* **17** 2245–60
- Brando P M, Goetz S J, Baccini A, Nepstad D C, Beck P S A and Christman M C 2010 Seasonal and interannual variability of climate and vegetation indices across the Amazon *Proc. Natl Acad. Sci. USA* **107** 14685–90
- Brienen R J W and Zuidema P A 2005 Relating tree growth to rainfall in Bolivian rain forests: a test for six species using tree ring analysis *Oecologia* **146** 1–12
- Chave J *et al* 2010 Regional and seasonal patterns of litterfall in tropical South America *Biogeosciences* **7** 43–55
- Chen J, Jonsson P, Tamurab M, Gaa Z, Matsushita B and Eklundh B 2004 A simple method for reconstructing a high-quality NDVI time-series data set based on the Savitzky–Golay filter *Remote Sens. Environ.* **91** 332–44
- Doughty C E and Goulden M L 2008 Seasonal patterns of tropical forest leaf area index and CO₂ exchange *J. Geophys. Res.* **113** G00B06

- Eva H D *et al* 2003 The land cover map for South America in the year 2000 *GLC2000 Database* (Ispra: European Commission Joint Research Centre)
- Galvão L S, Santos J R, Roberts D A, Breunig F M, Toomey M and Moura Y M 2011 On intra-annual EVI variability in the dry season of tropical forest: a case study with MODIS and hyperspectral data *Remote Sens. Environ.* **115** 2350–9
- Gond V *et al* 2011 Broad-scale spatial pattern of forest landscape types in the Guiana Shield *Int. J. Appl. Earth Obs. Geoinf.* **13** 357–67
- Gonsamo A, Chen J M, Price D T, Kurz W A and Wu C 2012 Land surface phenology from optical satellite measurement and CO₂ eddy covariance technique *J. Geophys. Res.* **117** G03032
- Green A A, Berman M, Switzer P and Craig M D 1988 A transformation for ordering multispectral data in terms of image quality with implications for noise removal *IEEE Trans. Geosci. Remote Sens.* **26** 65–74
- Huber O 2006 Herbaceous ecosystems on the Guayana Shield, a regional overview *J. Biogeogr.* **33** 464–75
- Huete A R, Didan K, Shimabukuro Y E, Ratana P, Saleska S R, Hutya L R, Yang W, Nemani R R and Myneni R 2006 Amazon rainforests green-up with sunlight in dry season *Geophys. Res. Lett.* **33** L06405
- IBGE (Instituto Brasileiro de Geografia e Estatística) 2004 *Mapa de Biomas do Brasil e o Mapa de Vegetação do Brasil* (Rio de Janeiro: Instituto Brasileiro de Geografia e Estatística) (available from www.ibge.gov.br/home/presidencia/noticias/21052004biomashtml.shtml)
- Jönsson P and Eklundh L 2002 Seasonality extraction by function fitting to time-series of satellite sensor data *IEEE Trans. Geosci. Remote Sens.* **40** 1824–32
- Juárez R I N, Hodnett M G, Fu R, Goulden M L and von Randow C 2007 Control of dry season evapotranspiration over the Amazonian forest as inferred from observations at a southern Amazon forest site *J. Clim.* **20** 2827–39
- Justiniano M J and Fredericksen T S 2000 Phenology of tree species in bolivian dry forests *Biotropica* **32** 276–81
- Kruse F A, Lefkoff A B, Boardman J B, Heidebrecht K B, Shapiro A T, Barloon P J and Goetz A F H 1993 The spectral image processing system (SIPS)—interactive visualization and analysis of imaging spectrometer data *Remote Sens. Environ.* **44** 145–63
- Liebmann B and Marengo J A 2001 Interannual variability of the rainy season and rainfall in the Brazilian Amazon basin *J. Clim.* **14** 4308–18
- López R P and Zambrana-Torrel C 2005 Representation of Andean dry ecoregions in the protected areas of Bolivia: the situation in relation to the new phytogeographical findings *Biodivers. Conserv.* **15** 2163–75
- Maignan F, Bréon F-M, Bacour C, Demarty J and Poirson A 2008 Interannual vegetation phenology estimates from global AVHRR measurements: comparison with *in situ* data and applications *Remote Sens. Environ.* **112** 496–505
- Malhado A C M, Costa M H, Lima F Z, Portilho K C and Figueiredo D N 2009 Seasonal leaf dynamics in an Amazonian tropical forest *Forest Ecol. Manag.* **258** 1161–5
- Marengo J A, Liebmann B, Kousky V E, Filizola N P and Wainer I C 2001 Onset and end of the rainy season in the Brazilian Amazon basin *J. Clim.* **14** 833–52
- Moles A T and Westoby M 2000 Do small leaves expand faster than large leaves, and do shorter expansion times reduce herbivore damage? *Oikos* **90** 517–24
- Myneni R B *et al* 2007 Large seasonal swings in leaf area of Amazon rainforest *Trans. R. Soc.* **1498** 1839–48
- Nebel G, Dragsted J and Vega A S 2001 Litter fall, biomass and net primary production in flood plain forests in the Peruvian Amazon *Forest Ecol. Manag.* **150** 93–102
- Norconk M A and Conklin-Brittain N L 2004 Variation on frugivory: the diet of Venezuelan white-faced sakis *Int. J. Primat.* **25** 1–26
- Panagos P, Jones A, Bosco C and Senthil Kumar P S 2011 European Digital Archive of Soil Maps (EuDASM): preserving important soil data for public free access *Int. J. Digital Earth* **4** 434–43
- Patino S, Fyllas N M, Baker T R, Paiva R, Quesada C A, Santos A J B and Lloyd J 2012 Coordination of physiological and structural traits in Amazon forest trees *Biogeosciences* **9** 775–801
- Peres C 1994 Primate responses to phenological change in Amazonian Terra Firme forest *Biotropica* **26** 98–112
- Pinto L P and Setz E Z F 2004 Diet of *Alouattabelzebul discolor* in an Amazonian rain forest of northern Mato Grosso State, Brazil *Int. J. Primat.* **25** 1197–211
- Pinzon J, Brown M E and Tucker C J 2005 Satellite time series correction of orbital drift artifacts using empirical mode decomposition *Hilbert–Huang Transform: Introduction and Applications* ed N E Huang and S S P Shen (Hackensack, NJ: World Scientific) pp 167–86
- Quesada C A *et al* 2009 Regional and large-scale patterns in Amazon forest structure and function are mediated by variations in soil physical and chemical properties *Biogeosci. Discuss.* **6** 3993–4057
- Rangel J, Lowy P D, Aguilar M and Garzón A 1997 Tipos de vegetación en Colombia *Colombia: Diversidad Biótica II* ed J Rangel, P D Lowy and M Aguilar (Bogotá: Guadalupe) pp 89–382
- Richardson A D, Keenan T F, Migliavacca M, Ryu Y, Sonnentag O and Toomey M 2013 Climate change, phenology, and phenological control of vegetation feedbacks to the climate system *Agric. Forest Meteorol.* **169** 156–73
- Rodell M *et al* 2004 The global land data assimilation system *Bull. Am. Meteorol. Soc.* **85** 381–94
- Saatchi S S, Nelson B, Podest E and Holt J 2000 Mapping land cover types in the Amazon basin using 1 km JERS-1 mosaic *Int. J. Remote Sens.* **21** 1201–34
- Saleska S R, Didan K, Huete A R and Rocha H R 2007 Amazon forests green-up during 2005 drought *Science* **318** 612
- Samanta A, Knyazikhin Y, Xu L, Dickinson R E, Fu R, Costa M H, Saatchi S S, Nemani R R and Myneni R B 2012 Seasonal changes in leaf area of Amazon forests from leaf flushing and abscission *J. Geophys. Res.* **117** G01015
- Schafer J S, Holben B N, Eck T F, Yamasoe M A and Artaxo P 2002 Atmospheric effects on insolation in the Brazilian Amazon: observed modification of solar radiation by clouds and smoke and derived single scattering albedo of fire aerosols *J. Geophys. Res.* **107** 8074
- Selva E C, Couto E G, Johnson M S and Lehmann J 2007 Litterfall production and fluvial export in headwater catchments of the southern Amazon *J. Trop. Ecol.* **23** 329–35
- Selvaradjou S-K, Montanarella L, Spaargaren O and Dent D 2005 *European Digital Archive of Soil Maps (EuDASM)—Soil Maps of Latin America and Caribbean Islands (EUR 21822 EN)* (Luxembourg: Office of the Official Publications of the European Communities)
- Silman M R 2007 Plant species diversity in Amazonian forests *Tropical Rainforest Responses to Climatic Change* ed M B Bush and J R Flenley (Chichester: Praxis Publishing) pp 269–94
- Sinimu G, Coley P D, Lemes M R, Lokvam J and Kursar T A 2012 Do the antiherbivore traits of expanding leaves in the Neotropical tree *Inga paraensis* (Fabaceae) vary with light availability? *Oecologia* **170** 669–76
- Sombroek W 2001 Spatial and temporal patterns of amazon rainfall: consequences for the planning of agricultural occupation and the protection of primary forests *Ambio* **30** 388–96

- Sternberg L D L 2001 Savanna-forest hysteresis in the tropics *Glob. Ecol. Biogeogr.* **10** 169–378
- ter Steege H *et al* 2006 Continental-scale patterns of canopy tree composition and function across Amazonia *Nature* **443** 444–7
- Tucker C J, Pinzon J E, Brown M E, Slayback D A, Pak E W, Mahoney D R, Vermote E F and Saleous N E 2005 An extended AVHRR 8 km NDVI dataset compatible with MODIS and SPOT vegetation NDVI data *Int. J. Remote Sens.* **26** 4485–98
- van Schaik C P, Terborgh J W and Wright S J 1993 The phenology of tropical forests: adaptative significance and consequences for primary consumers *Annu. Rev. Ecol. Syst.* **24** 353–77
- Wu C, Chen J M, Gonsamo A, Price D T, Black T A and Kurz W A 2012 Interannual variability of net carbon exchange is related to the lag between the end-dates of net carbon uptake and photosynthesis: evidence from long records at two contrasting forest stands *Agric. Forest Meteorol.* **164** 29–38
- Xiao X, Hagen S, Zhang Q, Keller M and Moore B III 2006 Detecting leaf phenology of seasonally moist tropical forests in South America with multi-temporal MODIS images *Remote Sens. Environ.* **103** 465–73
- Zhu Z, Bi J, Pan Y, Ganguly S, Anav A, Xu L, Samanta A, Piao S, Nemaniand R R and Myneni R B 2013 Global data sets of vegetation leaf area index (LAI)3g and fraction of photosynthetically active radiation (FPAR)3g derived from global inventory modeling and mapping studies (GIMMS) Normalized Difference Vegetation Index (NDVI)3g for the period 1981 to 2011 *Remote Sens.* **5** 927–48